

Modern Physics Letters A  
 © World Scientific Publishing Company

## RECENT SEARCHES FOR CONTINUOUS GRAVITATIONAL WAVES

KEITH RILES

*Physics Department, University of Michigan, 450 Church Street  
 Ann Arbor, Michigan 48109-1040, USA  
 kriles@umich.edu*

Received (17 November 2017)

Revised (Day Month Year)

Gravitational wave astronomy opened dramatically in September 2015 with the LIGO discovery of a distant and massive binary black hole coalescence. The more recent discovery of a binary neutron star merger, followed by a gamma ray burst and a kilonova, reinforces the excitement of this new era, in which we may soon see other sources of gravitational waves, including continuous, nearly monochromatic signals. Potential continuous wave (CW) sources include rapidly spinning galactic neutron stars and more exotic possibilities, such as emission from axion Bose Einstein “clouds” surrounding black holes. Recent searches in Advanced LIGO data are presented, and prospects for more sensitive future searches discussed.

*Keywords:* Gravitational waves; neutron star; pulsar; continuous wave; LIGO; Virgo

### 1. Introduction

LIGO’s detection in September 2015 of gravitational waves from the coalescence of heavy stellar-mass black holes (GW150914)<sup>1</sup> inaugurated observational gravitational wave astronomy, a new field ripe for discovery and one already deepening our understanding of astrophysics. The subsequent detections of additional binary black hole mergers GW151226,<sup>2</sup> GW170104,<sup>3</sup> GW170608,<sup>4</sup> and GW170814,<sup>5</sup> along with a binary neutron star merger<sup>6</sup> (last two events seen also by Virgo) associated with a short gamma ray burst (GRB)<sup>7</sup> and a kilonova<sup>8</sup> have confirmed the excitement of detecting gravitational wave transients.

An entirely different type of gravitational wave source merits attention too – continuous waves (CWs) emitted by compact spinning objects, most notably non-axisymmetric neutron stars in our own galaxy. Despite their relative closeness ( $\sim$ several kpc vs tens to hundreds of Mpc), such sources are expected to produce gravitational-wave strain amplitudes orders of magnitude weaker than those seen from compact binary mergers, *i.e.*,  $O(10^{-25})$  or smaller compared to  $O(10^{-21})$ . Our only hope of detecting such weak signals comes from integrating data over long time spans, but such integrations incur, in most searches, substantial computing

2 *K. Riles*

cost from covering finely a large parameter space volume (*e.g.*, frequency evolution, sky location, potential orbital parameters). In nearly every CW search, achievable sensitivity is limited by finite computational resources.

In the following, section 2 discusses both conventional and exotic potential sources of CW gravitational radiation, and section 3 presents a wide variety of searches tailored to *a priori* knowledge (or lack thereof) of the source properties, along with results (so far all negative) of those searches. Where available, results from recent searches in Advanced LIGO data will be presented; for ongoing searches not yet published, older results from Initial LIGO and Virgo searches will be presented instead. Finally, section 4 discusses the prospects for future searches in Advanced LIGO and Virgo data, as detector sensitivities and algorithms improve.

This brief review focuses on CW radiation potentially detectable with current-generation ground-based gravitational wave interferometers, which are sensitive in the audio band. Past and future searches for lower-frequency CW radiation from supermassive black hole binaries at  $\sim$ nHz frequencies using pulsar timing arrays<sup>9</sup> or from stellar-mass galactic binaries at  $\sim$ mHz frequencies using the space-based LISA<sup>10</sup> are not discussed here.

## 2. Potential CW Sources

In the frequency band of present ground-based detectors, the canonical sources of continuous gravitational waves are galactic, non-axisymmetric neutron stars spinning fast enough that their rotation frequencies (or twice their frequencies) are in the LIGO and Virgo detectable band. These nearby neutrons stars offer a “conventional” source of CW radiation – as astrophysically extreme as such objects are.

A truly exotic postulated source is a “cloud” of bosons, such as QCD axions, surrounding a fast-spinning black hole, bosons that can condense in gargantuan numbers to a small number of energy levels, enabling coherent gravitational wave emission from boson annihilation or from level transitions. Attention here focuses mainly on the conventional neutron stars, but the exotic boson cloud scenario is also discussed briefly.

### 2.1. *Fast-spinning neutron stars*

Spinning neutron stars could generate detectable gravitational waves via several possible mechanisms. Isolated neutron stars may exhibit intrinsic non-axisymmetry from residual crustal deformation (*e.g.*, from cooling & cracking of the crust),<sup>11</sup> from non-axisymmetric distribution of magnetic field energy trapped beneath the crust<sup>12</sup> or from a pinned neutron superfluid component in the star’s interior (see Ref. 13 for a discussion of emission from magnetic and thermal “mountains” and Refs. 14, 15 for recent, comprehensive reviews of GW emission mechanisms from neutron stars). Maximum allowed asymmetries depend on the neutron star equation of state<sup>16</sup> and on the breaking strain of the crust.<sup>17</sup>

Normal modes of oscillations could also arise, including  $r$ -modes in which quadrupole mass currents emit gravitational waves.<sup>18–21</sup> These  $r$ -modes can be inherently unstable, arising from azimuthal interior currents that are retrograde in the star’s rotating frame, but are prograde in an external reference frame. As a result, the quadrupolar gravitational wave emission due to these currents leads to an *increase* in the strength of the current. This positive-feedback loop leads to a potential intrinsic instability. The frequency of such emission is expected to be approximately 4/3 the rotation frequency.<sup>18–21</sup> Serious concerns have been raised,<sup>15,22</sup> however, about the detectability of the emitted radiation for young isolated neutron, where mode saturation appears to occur at low  $r$ -mode amplitudes because of various dissipative effects. A recent study,<sup>23</sup> however, is more optimistic about newborn neutron stars. The same authors, on the other hand, find that  $r$ -mode emission from millisecond pulsars is likely to be undetectable by Advanced LIGO.<sup>24</sup> The notion of a runaway rotational instability was first appreciated for high-frequency  $f$ -modes,<sup>30,31</sup> (Chandrasekhar-Friedman-Schutz instability), but realistic viscosity effects seem likely to suppress the effect in conventional neutron star production.<sup>32,33</sup> The  $f$ -mode stability could play an important role, however, for a supramassive or hypermassive neutron star formed as the remnant of a binary neutron star merger.<sup>34</sup>

In addition, as discussed below, a binary neutron star may experience direct non-axisymmetry from non-isotropic accretion<sup>35–37</sup> (also possible for an isolated young neutron star that has experienced fallback accretion shortly after birth), or may exhibit  $r$ -modes induced by accretion spin-up.

Given the various potential mechanisms for generating continuous gravitational waves from a spinning neutron star, detection of the waves should yield valuable information on neutron star structure and on the equation of state of nuclear matter at extreme pressures, especially when combined with electromagnetic observations of the same star.

In principle, there should be  $O(10^{8-9})$  neutron stars in our galaxy,<sup>38</sup> out of which only about 2500 have been detected, primarily as radio pulsars. This small fraction of detections is expected, for several reasons. Radio pulsations require high magnetic field and rotation frequency. An early study<sup>39,40</sup> implied the relation  $B \cdot f_{\text{rot}}^2 > 1.7 \times 10^{11} \text{ G} \cdot (\text{Hz})^2$  based on a model of radiation dominated by electron-positron pair creation in the stellar magnetosphere, a model broadly consistent with empirical observation, although the resulting “death line” in the plane of period and period derivative is perhaps better understood to be a valley.<sup>41</sup> As a result, isolated pulsars seem to have pulsation lifetimes of  $O(10^7 \text{ years})$ ,<sup>40</sup> after which they are effectively radio-invisible. On this timescale, they also cool to where thermal X-ray emission is difficult to detect. There remains the possibility of X-ray emission from steady accretion of interstellar medium (ISM), but it appears that the kick velocities from birth highly suppress such accretion<sup>42,43</sup> which depends on the inverse cube of the star’s velocity through the ISM.

A separate population of pulsars and non-pulsating neutron stars can be found in binary systems. In these binaries accretion from a non-compact companion star can

4 *K. Riles*

lead to “recycling,” in which a spun-down neutron star regains angular momentum from the infalling matter. The rotation frequencies achievable through this spin-up are impressive – the fastest known rotator is J1748-2446ad at 716 Hz.<sup>44</sup> One class of such systems is the set of low mass X-ray binaries (LMXBs) in which the neutron star ( $\sim 1.4 M_{\odot}$ ) has a much lighter companion ( $\sim 0.3 M_{\odot}$ )<sup>40</sup> that overfills its Roche lobe, spilling material onto an accretion disk surrounding the neutron star or possibly spilling material directly onto the star, near its magnetic polar caps. When the donor companion star eventually shrinks and decouples from the neutron star, the neutron star can retain a large fraction of its maximum angular momentum and rotational energy. Because the neutron star’s magnetic field decreases during accretion (through processes that are not well understood), the spin-down rate after decoupling can be very small.

Equating the rotational energy loss rate to magnetic dipole radiation losses, leads to the relation:<sup>45</sup>

$$\left(\frac{dE}{dt}\right)_{\text{mag}} = -\frac{\mu_0 M_{\perp}^2 \omega^4}{6\pi c^3}, \quad (1)$$

where  $\omega$  is the rotational angular speed,  $M_{\perp}$  is the component of the star’s magnetic dipole moment perpendicular to the rotation axis:  $M_{\perp} = M \sin(\alpha)$ , with  $\alpha$  the angle between the axis and north magnetic pole. In a pure dipole moment model, the magnetic pole field strength at the surface is  $B_0 = \mu_0 M / 2\pi R^3$ . Equating this energy loss to that of the (Newtonian) rotational energy  $\frac{1}{2} I_{zz} \omega^2$  leads to the prediction:

$$\frac{d\omega}{dt} = -\frac{\mu_0 R^6}{6\pi c^3 I_{zz}} B_{\perp}^2 \omega^3. \quad (2)$$

Note that the spin-down rate is proportional to the square of  $B_{\perp} = B_0 \sin(\alpha)$  and to the cube of the rotation frequency.

More generally, the spin-down rate is often taken to have a power law dependence:  $\dot{f} = K f^n$  for some negative constant  $K$  and exponent  $n$  that depends on the energy loss mechanism (*e.g.*, magnetic dipole emission:  $n = 3$ ; gravitational radiation:  $n = 5$  or  $n = 7$ , depending on mechanism). In this approximation, the age  $\tau$  of a neutron star can be related to its birth rotation frequency  $f_0$  and current frequency  $f$  by ( $n \neq 1$ ):

$$\tau = -\left[\frac{f}{(n-1)\dot{f}}\right] \left[1 - \left(\frac{f}{f_0}\right)^{(n-1)}\right], \quad (3)$$

and in the case that  $f \ll f_0$ ,

$$\tau \approx -\left[\frac{f}{(n-1)\dot{f}}\right]. \quad (4)$$

Assuming  $n$  (often called the “braking index” and derived from the ratio  $f\ddot{f}/\dot{f}^2$  when  $\ddot{f}$  is measurable) is three (magnetic dipole dominance), leads to approximate inferred ages for many binary radio pulsars in excess of  $10^9$  years and even well

over  $10^{10}$  years.<sup>46</sup> One calculation suggests that this surprising result can be explained by reverse-torque spin-down during the Roche lobe decoupling phase.<sup>47</sup> In fact, measured braking indices for even young pulsars tend to be less than three, suggesting that the model of a neutron star spinning down with constant magnetic field is, most often, inaccurate.<sup>40</sup> One recently reported exception, however, is X-ray pulsar J1640-4631 with a measured index of  $3.15 \pm 0.03$ .<sup>48</sup> See Ref. 49, 50 for discussions of spin-down evolution in the presence of both gravitational wave and electromagnetic torques. Other suggested mechanisms for less-than-3 braking indices are re-emerging buried magnetic fields and a decaying inclination angle between the magnetic dipole axis and the spin axis.<sup>51–53</sup> An interesting observation of the aftermath of two short GRBs noted indirectly inferred braking indices near or equal to three,<sup>54</sup> suggesting the rapid spin-down of millisecond magnetars, possibly born from neutron star mergers. (No direct evidence of a such a post-merger remnant has been observed from GW170817.<sup>55</sup>) It has been argued recently that the inter-glitch evolution of spin for the X-ray pulsar J0537-6910 displays behavior consistent with a braking index of 7,<sup>56</sup> which is expected for a spin-down dominated by  $r$ -mode emission.

Speaking broadly, one can identify three categories of neutron stars that are potentially detectable via continuous gravitational waves: relatively young, isolated stars with spin frequencies below  $\sim 50$  Hz, such as the Crab pulsar; actively accreting stars in binary systems; and recycled “millisecond” stars for which accretion has ceased and which generally have rotation frequencies above 100 Hz. In some cases the companion donor has disappeared, *e.g.*, via ablation, leaving an isolated neutron star, but most known millisecond pulsars remain in binary systems.<sup>46</sup>

Let’s now consider the gravitational radiation one might expect from these stars. If a star at a distance  $r$  away has a quadrupole asymmetry, parametrized by its ellipticity:

$$\epsilon \equiv \frac{I_{xx} - I_{yy}}{I_{zz}}, \quad (5)$$

and if the star is spinning about the approximate symmetry axis of rotation ( $z$ ), (assumed optimal – pointing toward the Earth), then the expected intrinsic strain amplitude  $h_0$  is

$$h_0 = \frac{4\pi^2 G I_{zz} f_{\text{GW}}^2}{c^4 r} \epsilon = (1.1 \times 10^{-24}) \left( \frac{I_{zz}}{I_0} \right) \left( \frac{f_{\text{GW}}}{1 \text{ kHz}} \right)^2 \left( \frac{1 \text{ kpc}}{r} \right) \left( \frac{\epsilon}{10^{-6}} \right), \quad (6)$$

where  $I_0 = 10^{38} \text{ kg}\cdot\text{m}^2$  ( $10^{45} \text{ g}\cdot\text{cm}^2$ ) is a nominal moment of inertia of a neutron star, and the gravitational radiation is emitted at frequency  $f_{\text{GW}} = 2 f_{\text{rot}}$ . The total power emission in gravitational waves from the star (integrated over all angles) is

$$\frac{dE}{dt} = -\frac{32 G}{5 c^5} I_{zz}^2 \epsilon^2 \omega^6 = -(1.7 \times 10^{33} \text{ J/s}) \left( \frac{I_{zz}}{I_0} \right)^2 \left( \frac{\epsilon}{10^{-6}} \right)^2 \left( \frac{f_{\text{GW}}}{1 \text{ kHz}} \right)^6. \quad (7)$$

6 *K. Riles*

For an observed neutron star of measured  $f$  and  $\dot{f}$ , one can define the “spin-down limit” on maximum detectable strain by equating the power loss in equation (7) to the time derivative of the (Newtonian) rotational kinetic energy:  $\frac{1}{2}I\omega^2$ , as above for magnetic dipole radiation. One finds:

$$\begin{aligned} h_{\text{spin-down}} &= \frac{1}{r} \sqrt{-\frac{5G}{2c^3} I_{zz} \frac{\dot{f}_{\text{GW}}}{f_{\text{GW}}}} \\ &= (2.5 \times 10^{-25}) \left( \frac{1 \text{ kpc}}{r} \right) \sqrt{\left( \frac{1 \text{ kHz}}{f_{\text{GW}}} \right) \left( \frac{-\dot{f}_{\text{GW}}}{10^{-10} \text{ Hz/s}} \right) \left( \frac{I_{zz}}{I_0} \right)}. \end{aligned} \quad (8)$$

Hence for each observed pulsar with a measured frequency spin-down and distance  $r$ , one can determine whether or not energy conservation even permits detection of gravitational waves in an optimistic scenario. Unfortunately, nearly all known pulsars have strain spin-down limits below what can be detected by the LIGO and Virgo detectors at current sensitivities, as discussed below.

A similarly optimistic limit based only on the age of a known neutron star of unknown spin frequency can also be derived. If one assumes a star is spinning down entirely due to quadrupolar gravitational radiation, then the energy loss for this *gravitar* satisfies equation (4) with a braking index of five (seven for  $r$ -mode emission). Assuming a high initial spin frequency, the star’s age then satisfies:

$$\tau_{\text{gravitar}} = -\frac{f}{4\dot{f}}.$$

If one knows the distance and the age of the star, *e.g.*, from the expansion rate of its visible nebula, then under the assumption that the star has been losing rotational energy since birth primarily due to gravitational wave emission, then one can derive the following frequency-independent age-based limit on strain:<sup>57</sup>

$$h_{\text{age}} = (2.2 \times 10^{-24}) \left( \frac{1 \text{ kpc}}{r} \right) \sqrt{\left( \frac{1000 \text{ yr}}{\tau} \right) \left( \frac{I_{zz}}{I_0} \right)}. \quad (9)$$

A notable example is the Compact Central Object (CCO) in the Cassiopeia A supernova remnant. Its birth aftermath may have been observed by Flamsteed<sup>58</sup> in 1680, and the expansion of the visible shell is consistent with that date. Hence Cas A, which is visible in X-rays but shows no pulsations, is almost certainly a very young neutron star at a distance of about 3.4 kpc. From the above equation, one finds an age-based strain limit of  $1.2 \times 10^{-24}$ , which is accessible to LIGO and Virgo detectors in their most sensitive band.

Derivations for similar indirect and age-based limits on the dimensionless  $r$ -mode emission amplitude  $\alpha$  can be found in Ref. 59.

A simple steady-state argument by Blandford<sup>60</sup> led to an early estimate of the maximum detectable strain amplitude expected from a population of isolated gravitars of a few times  $10^{-24}$ , independent of typical ellipticity values, in the optimistic scenario that most neutron stars become gravitars. A later detailed numerical simulation<sup>61</sup> revealed, however, that the steady-state assumption does not generally

hold, leading to ellipticity-dependent expected maximum amplitudes that can be 2-3 orders of magnitude lower in the LIGO band for ellipticities as low as  $10^{-9}$  and a few times lower for ellipticity of about  $10^{-6}$ .

Another approximate empirically determined strain limit can be defined for accreting neutron stars in binary systems, such as Scorpius X-1. The X-ray luminosity from the accretion is a measure of mass accumulation rate at the surface. As the mass rains down on the surface it can add angular momentum to the star, which in equilibrium may be radiated away in gravitational waves. Hence one can derive a torque-balance limit:<sup>19, 62, 63</sup>

$$h_{\text{torque}} = (5 \times 10^{-27}) \sqrt{\left(\frac{600 \text{ Hz}}{f_{\text{GW}}}\right) \left(\frac{\mathcal{F}_x}{10^{-8} \text{ erg/cm}^2/\text{s}}\right)}, \quad (10)$$

where  $\mathcal{F}_x$  is the observed energy flux at the Earth of X-rays from accretion. Note that this limit is independent of the distance to the star.

The notion of gravitational wave torque equilibrium is potentially important, given that the maximum observed rotation frequency of neutron stars in LMXBs is substantially lower than one might expect from calculations of neutron star breakup rotation speeds ( $\sim 1400$  Hz).<sup>64</sup> It has been suggested<sup>65</sup> that there is a “speed limit” governed by gravitational wave emission that governs the maximum rotation rate of an accreting star. In principle, the distribution of frequencies could have a quite sharp upper frequency cutoff, since the angular momentum emission is proportional to the 5th power of the frequency. For example, for an equilibrium frequency corresponding to a particular accretion rate, doubling the accretion rate would increase the equilibrium frequency by only about 15%. Note, however, that a non-GW speed limit may arise from interaction between the neutron star’s magnetosphere and an accretion disk.<sup>66–68</sup>

A number of mechanisms have been proposed by which the accretion leads to gravitational wave emission in binary systems. The simplest is localized accumulation of matter, *e.g.*, at the magnetic poles (assumed offset from the rotation axis), leading to a non-axisymmetry. One must remember, however, that matter can and will diffuse into the crust under the star’s enormous gravitational field. This diffusion of charged matter can be slowed by the also-enormous magnetic fields in the crust, but detailed calculations<sup>69</sup> indicate the slowing is not dramatic. Another proposed mechanism is excitation of *r*-modes in the fluid interior of the star,<sup>18–21</sup> with both steady-state emission and cyclic spin-up/spin-down possible.<sup>22, 70</sup> Intriguing, sharp lines consistent with expected *r*-mode frequencies were reported recently in the accreting millisecond X-ray pulsar XTE J1751–305<sup>25</sup> and in a thermonuclear burst of neutron star 4U 1636–536.<sup>26</sup> The inconsistency of the observed stellar spin-downs for these sources with ordinary *r*-mode emission, however, suggests that a different type of oscillation is being observed<sup>27</sup> or that the putative *r*-modes are restricted to the neutron star crust and hence gravitationally much weaker than core *r*-modes.<sup>28</sup> Another recent study<sup>29</sup> suggests that spin frequencies observed in accreting LMXB’s

are consistent with two sub-populations, where the narrow higher-frequency component ( $\sim 575$  Hz with standard deviation of  $\sim 30$  Hz) may signal an equilibrium driven by gravitational wave emission.

## 2.2. Axion clouds bound to black holes

A provocative idea receiving increased theoretical attention in recent years posits that dark matter is not only composed of electromagnetically invisible massive bosons, such as axions, but that such bosons could be disproportionately found in the vicinity of rapidly spinning black holes.<sup>71,72</sup> These bosons could, in principle, be spontaneously created via energy extraction from the black hole’s rotation<sup>73,74</sup> and form a Bose-Einstein “cloud” with nearly all of the quanta occupying a relatively small number of energy levels. For a cloud bound to a black hole, the approximate inverse-square law attraction outside the Schwarzschild radius leads to an energy level spacing directly analogous to that of the hydrogen atom. The number of quanta occupying the low-lying levels can be amplified enormously by the phenomenon of superradiance in the vicinity of a rapidly spinning black hole (angular momentum comparable to maximum allowed in General Relativity). The bosons in a non- $s$  ( $\ell > 0$ ) negative-energy state can be thought of as propagating in a well formed between an  $\ell$ -dependent centrifugal barrier at  $r > r_{\text{Schwarzschild}}$  and a potential rising toward zero as  $r \rightarrow \infty$ , where wave function penetration into the black hole ergosphere permits transfer of energy from the black hole spin<sup>75–77</sup> into the creation of new quanta.

Two particular gravitational wave emission modes of interest here can arise in the axion scenario, both potentially leading to intense coherent radiation.<sup>78</sup> In one mode, axions can annihilate with each other to produce gravitons with frequency double that corresponding to the axion mass:  $f_{\text{graviton}} = 2m_{\text{axion}}c^2/h$ . In another mode, emission occurs from level transitions of quanta in the cloud. This Bose condensation is most pronounced when the reduced Compton wavelength of the axion is comparable to but larger than the scale of the black hole’s Schwarzschild radius:

$$\frac{\lambda}{2\pi} = \frac{\hbar}{m_{\text{axion}}c} \gtrsim \frac{2GM_{\text{BH}}}{c^2} \quad \Rightarrow \quad m_{\text{axion}} \lesssim (7 \times 10^{-11} \text{ eV}/c^2) \frac{M_{\odot}}{M_{\text{BH}}}, \quad (11)$$

where  $\hbar$  and  $G$  are Planck’s and Newton’s constants. Given the many orders of magnitude uncertainty in, for example, axion masses that could account for dark matter,<sup>79</sup> the relatively narrow mass window accessible to currently feasible CW searches (1-2 orders of magnitude) makes searching for such an emission a classic example of “lamppost” physics, where one can only hope that nature places the axion in this lighted area of a vast parameter space.

In principle, searching for these potential CW sources requires no fundamental change in the search methods described below, but search optimization can be refined for the potentially very slow frequency evolution expected during both annihilation and level transition emission. In addition, for a known black hole location,



a directed search can achieve better sensitivity than an all-sky search. Note that for string axiverse models, however, the axion cloud<sup>71,72,80</sup> can experience significant self-interactions which can lead to appreciable frequency evolution of the signal and to uncertainty on that evolution, a complication less important for the postulated QCD axion.<sup>78</sup> One interesting suggestion includes the possibility that a black hole formed from the detected merger of binary black holes could provide a natural target for follow-up CW searches.<sup>81</sup> To date, no published searches have been tailored for a black hole axion cloud source, but existing (non-optimized) limits on neutron star emission can be reinterpreted as limits on such emission.<sup>78</sup> Recent studies<sup>82,83</sup> argue that the lack of detection of a stochastic gravitational radiation background from the superposition of extragalactic black holes already places significant limits on axion masses relevant to CW searches.

### 3. Search Methods and Results

As discussed in section 2, continuous-wave (CW) gravitational radiation detectable by ground-based detectors is expected most plausibly from rapidly spinning neutron stars in our galaxy. Search strategies for CW radiation depend critically upon the *a priori* knowledge one has about the source. It is helpful to classify CW searches into three broad categories:<sup>84,85</sup> 1) *targeted* searches in which the star's position and rotation frequency are known, *i.e.*, known radio, X-ray or  $\gamma$ -ray pulsars; 2) *directed* searches in which the star's position is known, but rotation frequency is unknown, *e.g.*, a non-pulsating X-ray source at the center of a supernova remnant; and 3) *all-sky* searches for unknown neutron stars. The volume of parameter space over which to search increases in large steps as one progresses through these categories. In each category a star can be isolated or binary. For 2) and 3) any unknown binary orbital parameters further increase the search volume. In all cases we expect (and have now verified from unsuccessful searches to date) that source strengths are very small. Hence one must integrate data over long observation times to have any chance of signal detection. How much one knows about the source governs the nature of that integration. In general, the greater that knowledge, the more computationally feasible it is to integrate data coherently (preserving phase information) over long observation times, for reasons explained below.

In theory, a definitive continuous-wave source detection can be accomplished with a single gravitational wave detector because the source remains on, allowing follow-up verification of the signal strength and of the distinctive Doppler modulations of signal frequency due to the Earth's motion (discussed below). Hence a relatively large number of CW searches were carried out with both bar detectors and interferometer prototypes in the decades even before the major 1st-generation interferometers began collecting data, with many additional searches carried out in Initial LIGO and Virgo data.<sup>85</sup> In the following, we focus mainly on the most recent results from Advanced LIGO's first observing run O1.

### 3.1. Targeted and narrowband searches for known pulsars

In *targeted* searches for known pulsars using measured ephemerides from radio, optical, X-ray or  $\gamma$ -ray observations valid over the gravitational wave observation time, one can apply corrections for phase modulation (or, equivalently, frequency modulation) due to the motion of the Earth (daily rotation and orbital motion), and in the case of binary pulsars, for additional source orbital motion. For the Earth's motion, one has a daily relative frequency modulation of  $v_{\text{rot}}/c \approx 10^{-6}$  and a much larger annual relative frequency modulation of  $v_{\text{orb}}/c \approx 10^{-4}$ . The pulsar astronomy community has developed a powerful and mature software infrastructure for measuring ephemerides and applying them in measurements, using the TEMPO 2 program.<sup>87</sup> The same physical corrections for the Sun's, Earth's and Moon's motions (and for the motion of other planets), along with general relativistic effects including gravitational redshift in the Sun's potential and Shapiro delay for waves passing near the Sun, have been incorporated into the LIGO and Virgo software libraries.<sup>88</sup>

Consider the model of a rotating rigid triaxial ellipsoid (model for a neutron star), for which the strain waveform detected by an interferometer can be written as

$$h(t) = F_+(t, \psi) h_0 \frac{1 + \cos^2(\iota)}{2} \cos(\Phi(t)) + F_\times(t, \psi) h_0 \cos(\iota) \sin(\Phi(t)), \quad (12)$$

where  $\iota$  is the angle between the star's spin direction and the propagation direction  $\hat{k}$  of the waves (pointing toward the Earth), where  $F_+$  and  $F_\times$  are the (real) detector antenna pattern response factors ( $-1 \leq F_+, F_\times \leq 1$ ) to the + and  $\times$  polarizations.  $F_+$  and  $F_\times$  depend on the orientation of the detector and the source, and on the polarization angle  $\psi$ .<sup>86</sup> Here,  $\Phi(t)$  is the phase of the signal.

The phase evolution of the signal can be usefully expanded as a truncated Taylor series:

$$\Phi(t) = \phi_0 + 2\pi \left[ f_s(T - T_0) + \frac{1}{2} \dot{f}_s(T - T_0)^2 + \frac{1}{6} \ddot{f}_s(T - T_0)^3 \right], \quad (13)$$

where

$$T = t + \delta t = t - \frac{\vec{r}_d \cdot \hat{k}}{c} + \Delta_{E\odot} - \Delta_{S\odot}. \quad (14)$$

Here,  $T$  is the time of arrival of a signal at the solar system barycenter (SSB),  $\phi_0$  is the phase of the signal at fiducial time  $T_0$ ,  $\vec{r}_d$  is the position of the detector with respect to the SSB, and  $\Delta_{E\odot}$  and  $\Delta_{S\odot}$  are solar system Einstein and Shapiro time delays, respectively.<sup>89</sup> In this expression  $f_s$  is the nominal instantaneous frequency of the gravitational wave signal [twice the star's rotation frequency<sup>90</sup> for a signal created by a rotating star's non-zero ellipticity, as in equations (5-6)].

Various approaches have been used in targeted searches in LIGO and Virgo data to date: 1) A time-domain heterodyne method<sup>91</sup> in which Bayesian posteriors are determined on the signal parameters that govern absolute phase, amplitude

and amplitude modulations; 2) a matched-filter method in which marginalization is carried out over unknown orientation parameters (“ $\mathcal{F}$ -statistic”);<sup>92,93</sup> and 3) a Fourier-domain determination of a “carrier” strength along with the strengths of two pairs of sidebands created by amplitude modulation from the Earth’s sidereal rotation of each detector’s antenna pattern (“5-Vector” method).<sup>94,95</sup>

Results from searches of each type<sup>96</sup> are shown in Figure 1, where method 1) was applied to 200 stars, and methods 2) and 3) were applied to 11 and 10 stars, respectively, for which the spin-down limit (equation 8) was likely to be beaten or approached, given the detector sensitivity. Highlights of these searches include setting a lowest upper limit on strain amplitude of  $1.6 \times 10^{-26}$  (J1918-0642), setting a lowest upper limit on ellipticity of  $1.3 \times 10^{-8}$  (J0636+5129) and beating the spin-down limit on 8 stars (J0205+6449, J0534+2200, J0835-4510, J1302-6350, J1813-1246, J1952+3252, J2043+2740, J2229+6114). Perhaps the most notable result was setting an upper limit on the Crab pulsar’s (J0534+2200) energy loss to gravitational radiation at a level of **0.2%** of the star’s total rotational energy loss inferred from measured rotational spin-down.

These upper limits assume the correctness of General Relativity in that antenna pattern calculations used in the searches assume two tensor polarizations in strain. Alternative theories of gravity can, in principle, support four additional polarizations (two scalar and two vector modes), which would lead to different antenna pattern sensitivities.<sup>97</sup> Searches have been carried out for evidence of signals from the 200 targeted pulsars above exhibiting these other polarizations, using the heterodyned data products. In no case was significant evidence of a non-standard signal seen, and upper limits were placed.<sup>98</sup>

The targeted-search upper limits in Figure 1 assume a fixed phase relation between stellar rotation (measured by electromagnetic pulses) and gravitational wave emission ( $f_s = f_{\text{rot}}$ ). To allow for a more general scenario, such as slight differential rotation of EM- and GW-emitting regions, searches have also been carried out for signals very near in parameter space to those expected from an ideal phase relation. These so-called “narrowband” searches allow a relative frequency deviation of  $O(10^{-3})$ . Results from searches for 11 stars with expected sensitivities near the spin-down limits have been obtained from O1 data.<sup>99</sup> In general, these limits are expected and found to be higher than the corresponding upper limits from targeted searches above because the increased parameter space search implies an additional trials factor. Nonetheless, this narrowband search beat the spin-down limit on the Crab (J0534+2200), Vela (J0835-4510) and J2229+6114.

### 3.2. Directed searches for isolated stars

Unlike targeted searches, where the phase evolution of the signal is (assumed to be) known precisely enough to permit a coherent integration over the full observation time, in a *directed* search one has limited or no information about the phase evolution of the source, while knowing precisely the sky location of the star. The implied

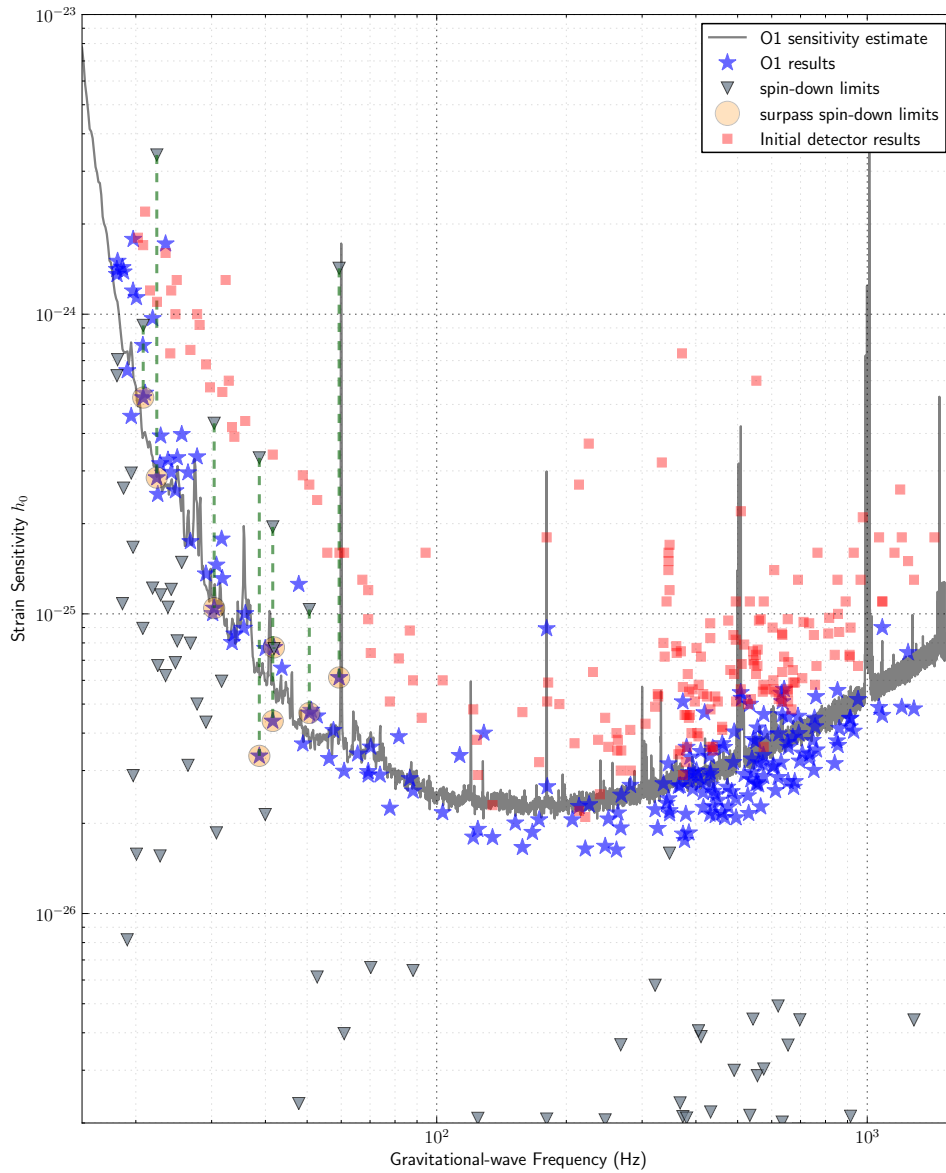


Fig. 1. Upper limits on  $h_0$  for known pulsars from searches in the LIGO O1 data.<sup>96</sup> The gray band shows the *a priori* estimated sensitivity range of the search. Also plotted are the lowest upper limits from searches in initial LIGO and Virgo data.

parameter space volume of the search will then depend sensitively upon the assumed age of the star. For a very young pulsar, one must search over not only the frequency and first frequency derivative (spin-down), but also over the second and possibly

higher derivatives.

To understand the scaling, imagine carrying out a coherent search, where one wishes to maintain phase coherence over the observation span  $T_{\text{obs}}$  of no worse than some error  $\Delta\Phi$ . From equation (13), one needs to search over  $f_s$  in steps proportional to  $1/T_{\text{obs}}$ , over  $\dot{f}_s$  in steps proportional to  $1/T_{\text{obs}}^2$ , and over  $\ddot{f}_s$  in steps proportional to  $1/T_{\text{obs}}^3$ . Hence a search that requires stepping in  $\ddot{f}_s$  will have a parameter space volume proportional to  $T_{\text{obs}}^6$ , with search time through the data incurring another power of  $T_{\text{obs}}$  in total computing cost (although accounting for the discreteness of the search over  $\ddot{f}_s$  reduces the power scaling for moderate  $T_{\text{obs}}$  values). Hence, even when the source direction is precisely known, the computational cost of a *coherent* search over  $f_s$ ,  $\dot{f}_s$  and  $\ddot{f}_s$  grows extremely rapidly with observation time. One can quickly exhaust all available computing capacity by choosing to search using a  $T_{\text{obs}}$  value that coincides with a full data set, *e.g.*, two years. In that case, one may simply choose the largest  $T_{\text{obs}}$  value with an acceptable computing cost, or one may choose instead a *semi-coherent* strategy of summing strain powers from many smaller time intervals, as discussed below in the context of all-sky searches. Both approaches have been used in recent years in analysis of Initial and Advanced LIGO data. As of this article's submission, no directed searches of Advanced LIGO data have been published, so here the focus will be on the final searches carried out in Initial LIGO data with a brief discussion of future prospects.

The coherent approach over tractable intervals<sup>57</sup> was applied to searches in the data from the last Initial LIGO data run (S6) for nine young Supernova remnants<sup>100</sup> and to a possible source at the core of the globular cluster NGC 6544.<sup>101</sup> In addition, the semi-coherent approach was applied in a computationally intensive Einstein@Home (see section 3.4) S6 search for continuous gravitational waves from the X-ray source at the center of the Cassiopeia supernova remnant,<sup>102</sup> which is especially interesting because of its youth, as discussed in section 2.1. Figure 2 shows the results of the Cas A search in comparison with the results from earlier searches, including from the coherent S6 search above,<sup>100</sup> from which it can be seen that the semi-coherent search, which exploits the full data set, achieves nearly a factor of two improvement in strain sensitivity. Note that these limits are roughly an order of magnitude higher, on the whole, than the limits achieved in the targeted search (Figure 1) using known ephemerides.

Another approach<sup>103</sup> for directed searches is based on cross correlation of independent data streams. The most straightforward method defines bins in detector-frame frequency and uses short coherence times, as in directional searches for stochastic gravitational radiation,<sup>104,105</sup> which can be used to search for both isolated and binary sources, albeit with limited sensitivity. One can use finer frequency binning, however, when correcting explicitly for Doppler modulation of the signal. Cross-correlation methods are especially robust against wrong assumptions about phase evolution and are attractive in searching for a very young object, such as a hypothetical neutron star remaining from Supernova 1987A (see Ref. 106 for a discussion of potential degradation of coherent searches from neutron star glitches).

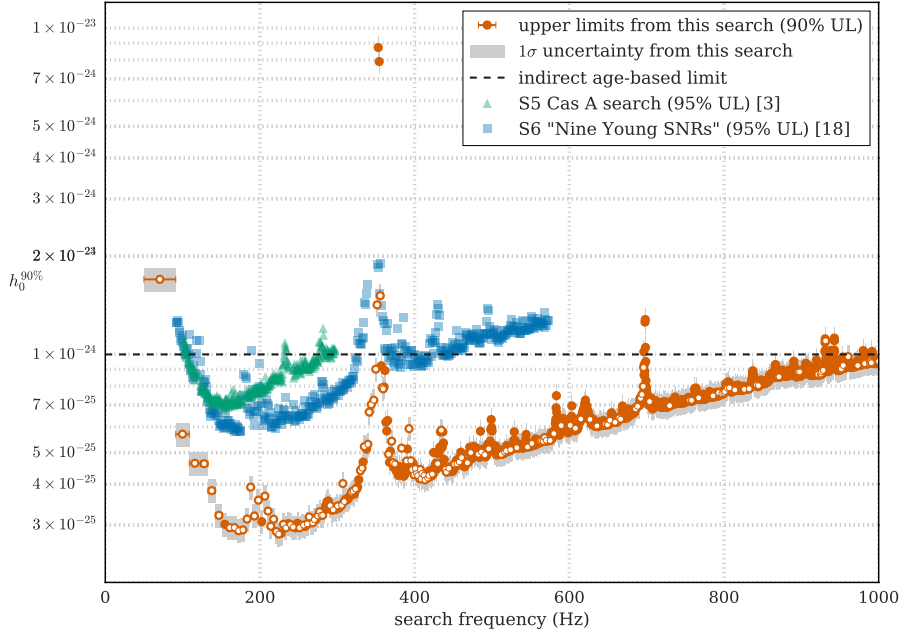


Fig. 2. Upper limits on  $h_0$  for Cassiopeia A from Initial LIGO S6 data,<sup>102</sup> shown with previous limits using the same or older data. Open circles indicate bands with partial contamination from instrumental disturbances.

In fact, a cross-correlation search for SN 1987A, including demodulation for effects from the motion of the Earth,<sup>107</sup> was carried out in Initial LIGO data<sup>108</sup> Recent application of cross-correlation methods to directed searches for binary sources will be discussed in the next section (3.3).

Directed searches for particular sources require making choices, that is, to prioritize among a wide set of potential targets in deciding how best to apply computational resources and analyst time. Recent work<sup>109,110</sup> has taken a Bayesian approach to address this problem, one that may be generalized to parameter choices in both directed and all-sky searches.

### 3.3. Directed searches for binary stars

For known binary pulsars with measured timing ephemerides, targeted searches work well, and upper limits have been reported for many stars, as described in section 3.1. But searching for known (possibly accreting) binary neutron stars not exhibiting pulsations or for entirely unknown binary stars once again significantly increases the parameter space, relative to the corresponding isolated star searches, posing new algorithmic challenges and computing costs.

Because of its high X-ray flux and the torque-balance relation for low-mass X-ray binaries [equation (10)], Scorpius X-1 is thought to be an especially promising search

target for advanced detectors and has been the subject of multiple searches in Initial and Advanced LIGO data. From equation (10), one expects a strain amplitude limited by<sup>111,112</sup>

$$h \sim (3.5 \times 10^{-26}) \left( \frac{600 \text{ Hz}}{f_{GW}} \right)^{\frac{1}{2}}. \quad (15)$$

While Sco X-1's rotation frequency remains unknown, its orbital period is well measured,<sup>113</sup> which allows substantial reduction in search space.

Searches for Sco X-1 in O1 data have been carried out with several methods: 1) a ‘‘Sideband’’ method<sup>114–117</sup> based on summing power in orbital sideband frequencies; 2) a non-demodulated cross-correlation methods<sup>105</sup> and 3) a demodulated cross-correlation method.<sup>118,119</sup> The demodulated cross-correlation method has proven to be the most sensitive method to date in such searches, as expected from a previous mock data challenge<sup>112</sup> including these methods and others,<sup>120–124</sup> and as shown in Figure 3, although computationally intensive methods using the  $\mathcal{F}$ -statistic may eventually improve upon it.<sup>125</sup> The strain upper limits shown in Figure 3 do not reach as low as the torque-balance benchmark in equation (15), but at Advanced LIGO design sensitivity and with longer data runs, future searches should begin to probe at least the low-frequency range of this benchmark. One complication in Sco X-1 searches is potential spin wandering due to fluctuations in accretion from its companion,<sup>127</sup> which limits the length of a coherence time that can be assumed safe for a signal template. One previous fully coherent search<sup>126</sup> restricted its coherence length to 10 days, to be conservative. Semi-coherent and cross-correlation methods<sup>104,116,118,122</sup> should be more robust against wandering, an expectation to be tested soon in a new mock data challenge.

It should be stated that obtaining more definitive information on the rotation frequency of Sco X-1 could potentially make the difference between missing and detecting its gravitational waves in advanced detector data, by reducing the statistical trials factor and thereby the threshold needed to identify an interesting outlier. *More intensive measurements and analysis of Sco X-1 X-ray emission could yield a dramatic scientific payoff.*

### 3.4. All-sky searches for isolated stars

In carrying out *all-sky* searches for unknown neutron stars, the computational considerations grow worse. The corrections for Doppler modulations and antenna pattern modulation due to the Earth's motion must be included, as for the targeted and directed searches, but the corrections are sky-dependent, and the spacing of the demodulation templates is dependent upon the inverse of the coherence time of the search. Specifically, for a coherence time  $T_{\text{coh}}$  the required angular resolution is<sup>128</sup>

$$\delta\theta \approx \frac{0.5 c \delta f}{f [v \sin(\theta)]_{\text{max}}}, \quad (16)$$

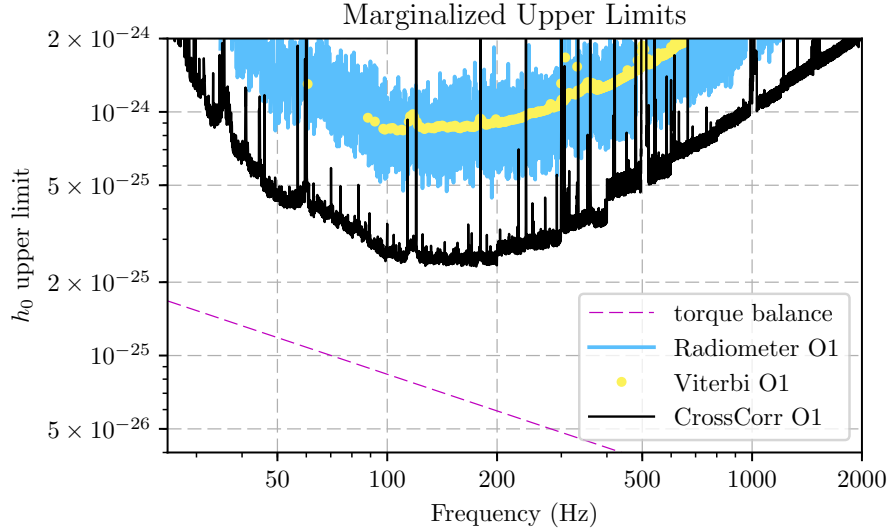
16 *K. Riles*


Fig. 3. Upper limits on  $h_0$  for Scorpius X-1 from Advanced LIGO O1 data, using several different search methods.<sup>119</sup> The dashed line indicates the torque-balance benchmark.

where  $\theta$  is the angle between the detector’s velocity relative to a nominal source direction, where the maximum relative frequency shift  $[v \sin(\theta)]_{\max}/c \approx 10^{-4}$ , and where  $\delta f$  is the size of the frequency bins in the search. For  $\delta f = 1/T_{\text{coh}}$ , one obtains:

$$\delta\theta \approx 9 \times 10^{-3} \text{ rad} \left( \frac{30 \text{ minutes}}{T_{\text{coh}}} \right) \left( \frac{300 \text{ Hz}}{f_s} \right), \quad (17)$$

where  $T_{\text{coh}} = 30$  minutes has been used in several all-sky searches to date. Because the number of required distinct points on the sky scales like  $1/(\delta\theta)^2$ , the number of search templates scales like  $(T_{\text{coh}})^2(f_s)^2$  for a fixed signal frequency  $f_s$ . Now consider attempting a search with a coherence time of 1 year for a signal frequency  $f_s = 1$  kHz. One obtains  $\delta\theta \sim 0.3 \mu\text{rad}$  and a total number of sky points to search of  $O(10^{14})$  – again, for a fixed frequency. Adding in the degrees of freedom to search over ranges in  $f_s$ ,  $\dot{f}_s$  and  $\ddot{f}_s$  makes a fully coherent 1-year all-sky search utterly impractical, given the Earth’s present total computing capacity.

As a result, tradeoffs in sensitivity must be made to achieve tractability in all-sky searches. The simplest tradeoff is to reduce the observation time to an acceptable coherence time. It can be more attractive, however, to reduce the coherence time still further to the point where the total observation time is divided into  $N = T_{\text{obs}}/T_{\text{coh}}$ , segments, each of which is analyzed coherently and the results added incoherently to form a detection statistic. One sacrifices intrinsic sensitivity per segment in the hope of compensating (partially) with the increased statistics from being able to use more total data, as discussed above for directed searches. In practice, for realistic



data observation spans (weeks or longer), the semi-coherent approach gives better sensitivity for fixed computational cost and hence has been used extensively in all-sky searches. One finds a strain sensitivity (threshold for detection) that scales approximately as the inverse fourth root of  $N$ .<sup>129</sup> Hence, for a fixed observation time, the sensitivity degrades roughly as  $N^{\frac{1}{4}}$  as  $T_{\text{coh}}$  decreases. This degradation is a price one pays for not preserving phase coherence over the full observation time, in order to make the search computationally tractable. An important virtue of semi-coherent searches methods is robustness with respect to deviations of a signal from an assumed coherent model.

Various semi-coherent algorithmic approaches have been tried, most based in some way on the “Stack Slide” algorithm<sup>130,131,151</sup> in which the power from Fourier transforms over each coherently analyzed segment is stacked on each other after sliding each transform some number of bins to account for Doppler modulation of the source frequency. One algorithm is a direct implementation of this idea called StackSlide.<sup>132</sup> Other implementations<sup>133,134</sup> are based on the Hough transform approach,<sup>135,136</sup> in which for each segment a detection statistic is compared to a threshold and given a weight of 0 or 1 (later refined to include adaptive non-unity weights, to account for variations in noise and detector antenna pattern<sup>137,138</sup>). The sums of those weights are accumulated in parameter space “maps,” with high counts warranting follow-up. The Hough approach offers, in principle, somewhat greater computational efficiency from reducing floating point operations, but its greater value lies in its robustness against non-Gaussian artifacts.<sup>128</sup> The Hough approach has been implemented in two distinct search pipelines, the “Sky Hough”<sup>133,139</sup> and “Frequency Hough”<sup>134,140,141</sup> programs, named after the different parameter spaces chosen in which to accumulate weight sums. Another implementation, known as PowerFlux,<sup>142–145</sup> improves upon the StackSlide method by weighting segments by the inverse variance of the estimated (usually non-stationary) noise and by searching explicitly over different assumed polarizations while including the antenna pattern correction factors in the noise weighting. Yet another method uses coincidences among  $\mathcal{F}$ -statistic outliers in multiple time segments typically longer than those used in the semi-coherent approaches.<sup>146,147</sup>

The deepest searches achieved to date have stacked  $\mathcal{F}$ -statistic values over time segments semi-coherently and have required the computational resources of the distributed computing project Einstein@Home<sup>148</sup> which uses the same software infrastructure (BOINC)<sup>149</sup> developed for the Seti@Home project.<sup>150</sup> The algorithms used in Einstein@Home have evolved steadily in sophistication and sensitivity over the last decade. Particular improvements have included search setup optimization,<sup>151,152</sup> more efficient semi-coherent stacking and template placement,<sup>153–159</sup> automated vetoing of instrumental lines,<sup>160,161</sup> and hierarchical outlier followup and veto.<sup>163–167</sup>

A recent comparison of these methods was carried out via a mock data challenge using initial LIGO data,<sup>168</sup> and these methods have been applied to published

searches of the Advanced LIGO O1 data set.<sup>169,170</sup> Figure 4 shows upper limits on strain from five searches (four covering 20-475 Hz and the deeper Einstein@Home covering 20-100 Hz with a smaller spin-down range). *Preliminary* upper limits,<sup>171</sup> from one of the pipelines (PowerFlux) are also shown for a broader frequency range in Figure 5, with results of comparable sensitivity from multiple pipelines expected to be published soon.

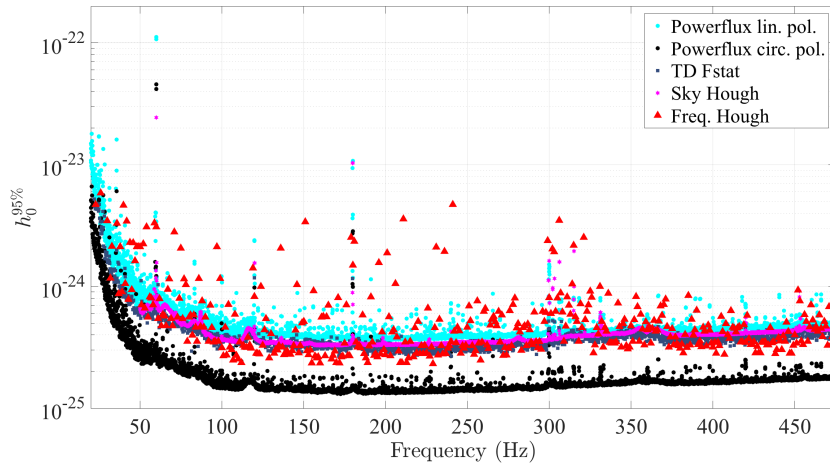


Fig. 4. All-sky upper limits on unknown sources of continuous waves from the Advanced LIGO O1 search,<sup>169</sup> based on five different search pipelines, as described in the text. Four pipelines cover the band 20-475 Hz, and the deepest search (Einstein@Home) covers the low-frequency band 20-100 Hz. The upper limits shown from the PowerFlux pipeline indicate the extremes between circular polarization (most optimistic) and worst-case linear polarization.

### 3.5. All-sky searches for binary stars

Given the computational difficulty in carrying out a search over the two unknown orbital parameters of a known binary star with known period and assumed circular orbit, it should come as no surprise that carrying out a search over three or more unknown orbital parameters for an unknown binary star anywhere in the sky is especially challenging. Several methods have been proposed for carrying out such an all-sky binary search, which approach the problem from opposite extremes. The first method, which has been used in a published search of Initial LIGO S6 data<sup>172</sup> is known as TwoSpect.<sup>120</sup> The program carries out a semi-coherent search over an observation time long compared to the maximum orbital period considered, while using coherence times short with respect to the orbital period. Fourier transforms are carried out over each row (fixed frequency bin) in a  $\sim$ year-long spectrogram

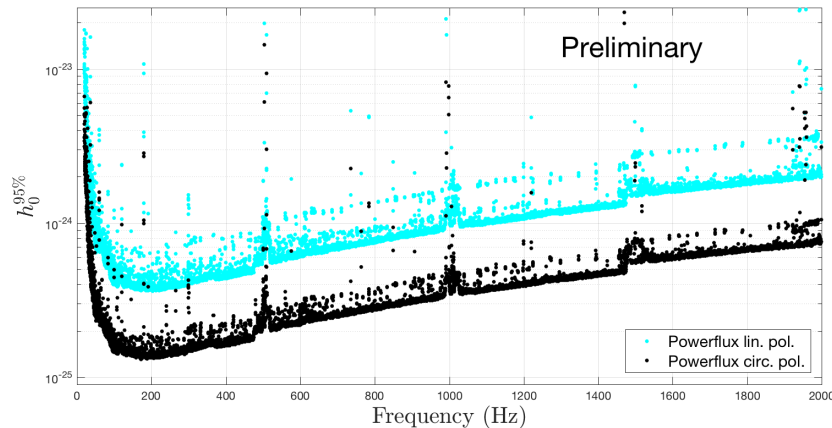


Fig. 5. Preliminary all-sky upper limits from the PowerFlux search pipeline over the band 20-2000 Hz on unknown sources of continuous waves from the Advanced LIGO O1 search.<sup>171</sup> As in the preceding figure, upper limits for circular and linear polarizations are shown separately.

and the resulting frequency-frequency plot searched for characteristic harmonic patterns. Another developed pipeline, known as Polynomial,<sup>124</sup> searches coherently using matched filters over an observation time short compared to the minimum orbital period considered. A bank of frequency polynomials in time is used for creating the matched filters, where for a small segment of an orbit, the frequency should vary as a low-order polynomial. Other proposed methods, which offer potentially substantial computational savings at a cost in sensitivity, include autocorrelations in the time-frequency plane<sup>173</sup> and stochastic-background techniques using skymaps with sidereal-day folding.<sup>174</sup> Results from one or more of these search methods applied to Advanced LIGO O1 data are expected in early 2018.

#### 4. Prospects for the Future

Over the next several years, the Advanced LIGO and Virgo detectors are expected to approach their design sensitivities in strain, improving by about another factor of three over current broadband sensitivities.<sup>175</sup> This dramatic improvement in strain increases the volume of the galaxy searched with CW pipelines by a factor between 9 and 27, depending on assumed neutron star ellipticities, signal frequencies, *etc.*, thereby increasing detection likelihood. As search ranges approach the dense galactic core, detection chances may rise more rapidly. In parallel to detector improvement, algorithms continue to improve, as researchers find more effective tradeoffs between computational cost and detection efficiency, while Moore's Law, including Graphical Processing Unit (GPU) exploitation, ensures increased computing resources for searches. All of these trends are encouraging for successful CW detection.

At the same time, theoretical uncertainties on what sensitivity is needed for the first CW detection are very large. While the spin-down limits based on gravitar assumptions and on either energy conservation or known age have been beaten for a handful of sources and will be beaten for more sources in the coming years, the gravitar model is surely optimistic – most stellar spin-downs are likely dominated by electromagnetic interactions. Whether the first detection is imminent or still many years distant remains unclear.

Electromagnetic astronomers could prove pivotal in hastening detection by identifying new nearby or young neutron stars, or discovering pulsations from known stars, perhaps most usefully from the accreting Sco X-1 system. Given the computational challenges of most CW searches, narrowing the parameter space of a search exploiting electromagnetic observations could make the difference between a gravitational wave miss and a discovery.

### Acknowledgments

The author is deeply grateful to colleagues in the LIGO Scientific Collaboration and Virgo collaboration Continuous Waves Search Group for close collaboration from which he has benefited in preparing this article. The author also thanks Cristiano Palomba, David Keitel, Maria Alessandra Papa, Karl Wette and John Whelan for helpful suggestions concerning the manuscript and thanks LIGO, Virgo and the Albert Einstein Institute for the use of figures. This work was supported in part by National Science Foundation Award PHY-1505932.

### References

1. B. Abbott *et al.*, *Phys. Rev. Lett.* **116** 131103 (2016).
2. B. Abbott *et al.*, *Phys. Rev. Lett.* **116** 241103 (2016).
3. B. Abbott *et al.*, *Phys. Rev. Lett.* **118** 221101 (2017).
4. B. Abbott *et al.*, to appear in *Astroph. J. Lett.*, arXiv:1711.05578, November 2017.
5. B. Abbott *et al.*, *Phys. Rev. Lett.* **119** 141101 (2017).
6. B. Abbott *et al.*, *Phys. Rev. Lett.* **119** 161101 (2017).
7. B. Abbott *et al.*, *Astroph. J. Lett.* **848** L13 (2017).
8. B. Abbott *et al.*, *Astroph. J. Lett.* **848** L12 (2017).
9. R.N. Manchester, in *Proceedings of the 12th Marcel Grossman Meeting*, Paris, August 2009, World Scientific.
10. P. Bender *et al.*, MPQ Reports, MPQ-208 (Max-Planck-Institut für Quantenoptik, Garching 1996);  
URL: <https://www.elisascience.org>.
11. V.R. Pandharipande, D. Pines and R.A. Smith, *Astroph. J.* **208** 550 (1976).
12. M. Zimmermann, *Nature* **271** 524 (1978).
13. B. Haskell *et al.*, *Mon. Not. Roy. Astron. Soc.* **450** 2393 (2015).
14. P. Lasky, *Pubs. Astron. Soc. Australia* **32** 34 (2015).
15. K. Glampedakis and L. Gualtieri, chapter in “Physics and Astrophysics of Neutron Stars”, NewCompStar COST Action 1304 (2017).
16. N.K. Johnson-McDaniel and B.J. Owen, *Phys. Rev. D* **88** 044004 (2013).
17. C.J. Horowitz and K. Kadau, *Phys. Rev. Lett.* **102** 191102 (2009).

18. N. Andersson, *Astroph. J.* **502** 708 (1998).
19. L. Bildsten, *Astroph. J. Lett.* **501** L89 (1998).
20. J.L. Friedman and S.M. Morsink, *Astroph. J.* **502** 714 (1998).
21. B.J. Owen *et al.*, *Phys. Rev. D* **58** 084020 (1998).
22. P. Arras *et al.*, *Astroph. J.* **591** 1129 (2003).
23. M. Alford and K. Schwenzer, *Astroph. J.* **781** 26 (2014).
24. M. Alford and K. Schwenzer, *Mon. Not. Roy. Astron. Soc* **446** 3631 (2015).
25. T. Strohmayer and S. Mahmoodifar, *Astroph. J.* **784** 72 (2014).
26. T. Strohmayer and S. Mahmoodifar, *Astroph. J.* **793** 2 (2014).
27. N. Andersson, D.I. Jones and W.C.G. Ho, *Mon. Not. Roy. Astron. Soc* **442** 1786 (2014).
28. U. Lee, *Mon. Not. Roy. Astron. Soc* **442** 3037 (2014).
29. A. Patruno, B. Haskell and N. Andersson, *Astroph. J.* **850** 106 (2017).
30. S. Chandrasekhar, *Phys. Rev. Lett.* **24** 611 (1970).
31. J.L. Friedman and B.F. Schutz, *Astroph. J.* **222** 281 (1978).
32. L. Lindblom and S.L. Detweiler, *Astroph. J.* **211** 565 (1977).
33. L. Lindblom and G. Mendell, *Astroph. J.* **444** 804 (1995).
34. D. Doneva, K.D. Kokkotas and P. Pnigouras, *Phys. Rev. D* **92** 104040 (2015).
35. B.J. Owen, *Phys. Rev. Lett.* **95** 211101 (2005).
36. G. Ushomirsky, C. Cutler and L. Bildsten, *Mon. Not. Roy. Astron. Soc* **319** 902 (2000).
37. A. Melatos and D.J.B. Payne, *Astroph. J.* **623** 1044 (2005).
38. R. Narayan, *Astroph. J.* **319** 162 (1987).
39. M. Ruderman & P. Sutherland, *Astroph. J.* **196** 51 (1975).
40. A. Lyne and F. Graham-Smith *Pulsar Astronomy*, 3rd edition (Cambridge University Press, Cambridge 2006).
41. B. Zhang, A.K. Harding and A.G. Muslimov, *Astroph. J. Lett.* **531** L135 (2000).
42. F. Hoyle and R.A. Lyttleton, *Proc. Cam. Phil. Soc.* **35** 405 (1939).
43. H. Bondi and F. Hoyle, *Mon. Not. Roy. Astron. Soc* **104** 273 (1944).
44. J.W. Hessels *et al.* *Science* **311** 1901 (2006).
45. F. Pacini, *Nature* **219** 145 (1968).
46. The Australia National Telescope Facility Pulsar Catalog is hosted here: URL: <http://www.atnf.csiro.au/people/pulsar/psrcat/>.
47. T.M. Tauris, *Science* **335** 561 (2012).
48. R.F. Archibald *et al.*, *Astroph. J. Lett.* **819** L16 (2016).
49. C. Palomba, *Astron. & Astroph.* **354** 163 (2000).
50. C. Palomba, *Mon. Not. Roy. Astron. Soc* **359** 1150 (2005).
51. T.M. Tauris and S. Konar, *A&A* **376** 543 (2001).
52. W. Ho, *Mon. Not. Roy. Astron. Soc* **452** 845 (2015).
53. S. Johnston and A. Karastergiou, *Mon. Not. Roy. Astron. Soc* **467** 3493 (2017).
54. P.D. Lasky *et al.*, *Astroph. J. Lett.* **843** L1 (2017).
55. B. Abbott *et al.*, *Astroph. J. Lett.* **851** L16 (2017).
56. N. Andersson *et al.*, submitted to *Astroph. J.*, arXiv:1711.05550, November 2017.
57. K. Wette *et al.*, *Class. Quant. Grav.* **25** 235011 (2008).
58. D.W. Hughes, *Nature* **285** 132 (1980).
59. B.J. Owen, *Phys. Rev. D* **82** 104002 (2010).
60. K.S. Thorne, in *300 Years of Gravitation*, eds. S.W. Hawking and W. Israel (Cambridge University Press, Cambridge 1987).
61. B. Knispel and B. Allen, *Phys. Rev. D* **78** 044031 (2008).
62. R.V. Wagoner, *Astroph. J.* **278** 345 (1984).
63. J. Papaloizou and J.E. Pringle *Mon. Not. Roy. Astron. Soc* **184** 501 (1978).

22 *K. Riles*

64. G.B. Cook, S.L. Shapiro and S.A. Teukolsky, *Astroph. J.* **424** 823 (1994).
65. D. Chakrabarty, *Nature* 424442003.
66. P. Ghosh and F.K. Lamb, *Astroph. J.* **234** 296 (1979).
67. B. Haskell and A. Patruno, *Astroph. J. Lett.* **738** L14 (2011).
68. A. Patruno, B. Haskell and C. D’Angelo, *Astroph. J.* **746** 9 (2012).
69. M. Vigelius and A. Melatos, *Astroph. J.* **717** 404 (2010).
70. Y. Levin, *Astroph. J.* **517** 328 (1999).
71. A. Arvanitaki *et al.*, *Phys. Rev. D* **81** 123530 (2010).
72. A. Arvanitaki and S. Dubovsky, *Phys. Rev. D* **83** 044026 (2011).
73. R. Penrose, *Riv. Nuovo Cim.* **1** 252 (1969).
74. D. Christodoulou, *Phys. Rev. Lett.* **25** 1596 (1970).
75. Ya. B. Zeldovich, *JETPL* **14** 180 (1971).
76. C. W. Misner, *Phys. Rev. Lett.* **28** 994 (1972).
77. A.A. Starobinskii, *JETP* **37** 28 (1973).
78. A. Arvanitaki, M. Baryakhtar and X. Huang, *Phys. Rev. D* **91** 084011 (2015).
79. G. Bertone, “Particle Dark Matter” (Cambridge University Press, 2010).
80. H. Kodama and H. Yoshino, *Prog. Theor. Exp. Phys.* **2014** 043E02 (2014).
81. A. Arvanitaki *et al.*, *Phys. Rev. D* **95** 043001 (2017).
82. R. Brito *et al.*, *Phys. Rev. Lett.* **119** 131101 (2017).
83. R. Brito *et al.*, *Phys. Rev. D* **96** 064050 (2017).
84. R. Prix, ASSL, Vol. 357, 651 (2009) “Gravitational Waves from Spinning Neutron Stars,” ed. W. Becker (Springer Berlin Heidelberg).
85. K. Riles, *Prog. Part. Nuc. Phys.* **68** 1 (2013).
86. B. Abbott *et al.*, *Phys. Rev. D* **69** 082004 (2004).
87. URL: <http://www.atnf.csiro.au/research/pulsar/tempo/>.
88. URL: <http://www.lsc-group.phys.uwm.edu/lal/>.
89. J.H. Taylor, *Phil. Trans. R. Soc. Lon. A* **341** 117 (1992).
90. M. Zimmermann and E. Szedenits, Jr., *Phys. Rev. D* **20** 351 (1979).
91. R. Dupuis and G. Woan, *Phys. Rev. D* **72** 102002 (2005).
92. P. Jaranowski, A. Królak and B.F. Schutz, *Phys. Rev. D* **58** 063001 (1998).
93. P. Jaranowski and A. Królak, *Class. Quant. Grav.* **27** 94015 (2010).
94. P. Astone *et al.*, *Class. Quant. Grav.* **27** 194016 (2010).
95. P. Astone *et al.*, *J. Phys. Conf. Ser.* **363** 012038 (2012).
96. B. Abbott *et al.*, *Astroph. J.* **839** 12 (2017).
97. M. Isi *et al.*, *Phys. Rev. D* **91** 082002 (2015).
98. B. Abbott *et al.*, to appear in *Phys. Rev. Lett.*, arxiv:1709.09203, September 2017.
99. B. Abbott *et al.*, to appear in *Phys. Rev. D*, arxiv:1710.02327, October 2017.
100. J. Aasi *et al.*, *Astroph. J.* **813** 39 (2015).
101. B. Abbott *et al.*, *Phys. Rev. D* **95** 082005 (2017).
102. S.J. Zhu *et al.*, *Phys. Rev. D* **94** 082008 (2016).
103. S. Dhurandhar *et al.*, *Phys. Rev. D* **77** 082001 (2008).
104. S.W. Ballmer, *Class. Quant. Grav.* **23** S179 (2006).
105. B. Abbott *et al.*, *Phys. Rev. Lett.* **118** 121102 (2017).
106. G. Ashton, R. Prix and D.I. Jones, *Phys. Rev. D* **96** 063004 (2017).
107. C. Chung *et al.*, *MNRAS* **414** 2650 (2011).
108. L. Sun *et al.*, *Phys. Rev. D* **94** 082004 (2016).
109. J. Ming *et al.*, *Phys. Rev. D* **93** 064011 (2016).
110. J. Ming *et al.*, submitted to *Phys. Rev. D*, arXiv:1708.02173, August 2017.
111. B. Abbott *et al.*, *Phys. Rev. D* **76** 082001 (2007).
112. C. Messenger *et al.*, *Phys. Rev. D* **92** 023006 (2015).

113. E.W. Gottlieb, E.L. Wright and W. Liller, *Astroph. J. Lett.* **195** L33 (1975).
114. C. Messenger and G. Woan, *Class. Quant. Grav.* **24** S469 (2007).
115. L. Sammut *et al.*, *Phys. Rev. D* **89** 043001 (2014).
116. S. Suvorova *et al.*, *Phys. Rev. D* **93** 123009 (2016).
117. B. Abbott *et al.*, *Phys. Rev. D* **95** 122003 (2017).
118. J.T. Whelan *et al.*, *Phys. Rev. D* **91** 102005 (2015).
119. B. Abbott *et al.*, *Astroph. J.* **841** 47 (2017).
120. E. Goetz and K. Riles, *Class. Quant. Grav.* **28** 215006 (2011).
121. E. Goetz and K. Riles, *Class. Quant. Grav.* **33** 085007 (2016).
122. G.D. Meadors, E. Goetz and K. Riles, *Class. Quant. Grav.* **33** 105017 (2016).
123. G.D. Meadors *et al.*, *Phys. Rev. D* **95** 042005 (2017).
124. S. van der Putten *et al.*, *J. Phys. Conf. Ser.* **228** 012005 (2010).
125. P. Leaci and R. Prix, *Phys. Rev. D* **91** 102003 (2015).
126. , J. Aasi *et al.*, *Phys. Rev. D* **91** 062008 (2015).
127. A. Mukherjee, C. Messenger and K. Riles, submitted to *Phys. Rev. D*, arXiv:1710.06185, October 2017.
128. B. Abbott *et al.*, *Phys. Rev. D* **77** 022001 (2008).
129. B. Abbott *et al.*, *Phys. Rev. D* **72** 2005 (102004).
130. P. Brady *et al.*, *Phys. Rev. D* **57** 2101 (1998).
131. P. Brady and T. Creighton, *Phys. Rev. D* **61** 082001 (2000).
132. G. Mendell and M. Landry, LIGO Report T050003 (January 2005).
133. B. Krishnan *et al.*, *Phys. Rev. D* **70** 082001 (2004).
134. F. Antonucci *et al.*, *Class. Quant. Grav.* **25** 184015 (2008).
135. P.V.C. Hough, in Proceedings of International Conference on High Energy Accelerators and Instrumentation, CERN (1959).
136. P.V.C. Hough, U.S. Patent 3,069,654 (1962).
137. C. Palomba *et al.*, *Class. Quant. Grav.* **22** S1255 (2005).
138. A.M. Sintes and B. Krishnan, *J. Phys. Conf. Ser.* **32** 206 (2006).
139. J. Aasi *et al.*, *Class. Quant. Grav.* **31** 085014 (2014).
140. P. Astone *et al.*, *Phys. Rev. D* **90** 042002 (2014).
141. J. Aasi *et al.*, *Phys. Rev. D* **93** 042007 (2016).
142. V. Dergachev, LIGO Report T050186 (September 2005).
143. V. Dergachev and K. Riles, LIGO Report T050187 (September 2005).
144. V. Dergachev, *Class. Quant. Grav.* **27** 205017 (2010).
145. V. Dergachev, *Phys. Rev. D* **87** 062001 (2013).
146. P. Astone *et al.*, *Phys. Rev. D* **82** 022005 (2010).
147. J. Aasi *et al.*, *Class. Quant. Grav.* **31** 165014 (2014).
148. B. Abbott *et al.*, *Phys. Rev. D* **79** 022001 (2009).
149. The Einstein@Home project is built upon the BOINC (Berkeley Open Infrastructure for Network Computing) architecture described at <http://boinc.berkeley.edu/>.
150. D.P. Anderson *et al.*, *Commun. A.C.M.* **45** 56 (2002).
151. C. Cutler, I. Gholami and B. Krishnan, *Phys. Rev. D* **72** 042004 (2005).
152. M. Shaltev, *Phys. Rev. D* **93** 044058 (2016).
153. R. Prix, *Phys. Rev. D* **75** 023004 (2007).
154. H.J. Pletsch, *Phys. Rev. D* **78** 102005 (2008) (.)
155. H.J. Pletsch and B. Allen, *Phys. Rev. Lett.* **103** 181102 (2009)
156. K. Wette and R. Prix, *Phys. Rev. D* **88** 123005 (2013).
157. K. Wette, *Phys. Rev. D* **90** 122010 (2014).
158. K. Wette, *Phys. Rev. D* **92** 082003 (2015).
159. K. Wette, *Phys. Rev. D* **94** 122002 (2016).

24 *K. Riles*

160. D. Keitel *et al.*, *Phys. Rev. D* **89** 064023 (2014).
161. D. Keitel and R. Prix, *Class. Quant. Grav.* **32** 035004 (2015).
162. D. Keitel, *Phys. Rev. D* **93** 084024 (2016).
163. R. Prix and M. Shaltev, *Phys. Rev. D* **85** 084010 (2012)
164. M. Shaltev *et al.*, *Phys. Rev. D* **89** 124030 (2014).
165. M.A. Papa *et al.*, *Phys. Rev. D* **94** 122006 (2016).
166. A. Singh *et al.*, *Phys. Rev. D* **96** 082003 (2017).
167. S.J. Zhu, M.A. Papa and S. Walsh, *Phys. Rev. D* **96** 124007 (2017).
168. S. Walsh *et al.*, *Phys. Rev. D* **94** 124010 (2016).
169. B. Abbott *et al.*, *Phys. Rev. D* **96** 062002 (2017).
170. B. Abbott *et al.*, to appear in *Phys. Rev. D*, arXiv:1707.02669, July 2017.
171. V. Dergachev for the LIGO Scientific Collaboration and Virgo Collaboration, presentation at the American Physical Society meeting, Washington, D.C., January 2017, LIGO-G1601939.
172. J. Aasi *et al.*, *Phys. Rev. D* **90** 062010 (2014).
173. A. Vicere and M. Yvert, *Class. Quant. Grav.* **33** 165006 (2016).
174. E. Thrane *et al.*, *Phys. Rev. D* **91** 124012 (2017).
175. B. Abbott *et al.*, *Liv. Rev. Rel.* **19** 1 (2016).